




Transcriptomic analysis and epigenetic regulators in human oocytes at different stages of oocyte meiotic maturation

Carla Caniçais^{a,b}, Daniel Sobral^d, Sara Vasconcelos^a, Mariana Cunha^c, Alice Pinto^f,
Joana Mesquita Guimarães^f, Fátima Santos^{f,1}, Alberto Barros^{a,c,e}, Sofia Dória^{a,b,2},
C. Joana Marques^{a,g,1,2,*} 

^a Genetics Unit, Department of Pathology, Faculty of Medicine University of Porto (FMUP), 4200-319, Portugal

^b ICBAS- School of Medicine and Biomedical Sciences, University of Porto, 4050-313, Porto, Portugal

^c Centre for Reproductive Genetics A Barros (CGRAB), 4100-009, Porto, Portugal

^d Genomics and Bioinformatics Unit, Department of Infectious Diseases, National Institute of Health Doutor Ricardo Jorge (INSA), 1649-016, Lisbon, Portugal

^e PROCRIAR Fertility Clinic, 4100-130, Porto, Portugal

^f Epigenetics Programme, The Babraham Institute, Cambridge, CB22 3AT, UK

^g CINTESIS@RISE-Health, Faculty of Medicine, University of Porto, Alameda Professor Hernâni Monteiro, 4200-319, Porto, Portugal

ARTICLE INFO

Keywords:
Oocytes
Oogenesis
Meiosis
Transcriptome
Epigenetics
RNA-Seq

ABSTRACT

Human oocytes are highly specialized cells with the capacity to store and regulate mRNAs during oocyte maturation, in preparation for post-fertilization steps.

Here we performed single-oocyte transcriptomic analysis of human oocytes in three meiotic maturation stages – Germinal Vesicle (GV; n = 6), Metaphase I (MI; n = 6) and Metaphase II (MII; n = 7).

Single-oocyte transcriptomic analysis revealed that the total number of expressed genes progressively decreased from GV to MII stages, with 9660 genes being transcribed in GV, 8734 in MI and 5889 in MII. The same tendency was observed for the number of uniquely expressed genes, with 1328 uniquely expressed genes in GV, 401 in MI and 72 in MII. GO analysis of the uniquely expressed genes showed distinct terms in GV oocytes such as transferase activity, organonitrogen compound metabolic process and ncRNA processing. Analysis of Differentially Expressed Genes (DEGs) between the three maturation stages revealed 1165 DEGs between GV and MII oocytes, with 635 being upregulated and 528 downregulated, 42 DEGs between GV and MI, with 38 being upregulated and 4 downregulated, and no significant changes in gene expression between MI and MII oocytes. Comprehensive analysis of epigenetic regulators showed high expression of several histone-modifying enzymes, namely deacetylases, acetylases, lysine demethylases and methyltransferases, and DNA methylation regulators, namely the maintenance methyltransferase *DNMT1* and its co-regulators *DPPA3* and *UHRF1*. Some of these epigenetic regulators were differentially expressed between maturation stages, namely *SIRT3*, *SIRT6*, *KDM3AP1*, *KMT2E*, *DNMT1*, *DPPA3* and the *MEST* and *RASGRF1* imprinted genes.

Our study contributes with important information on the transcriptional landscape of human oocytes in different stages of meiotic maturation, providing important insights into candidate biomarkers of human oocyte quality.

1. Introduction

Human oocytes undergo complex cellular and molecular changes that are essential for the success of fertilization and embryo

development. It has long been shown that these changes involve highly coordinated nuclear and cytoplasmic processes that take place during oocyte maturation (Eppig et al., 1996). Maturation of the oocyte involves three morphologically distinct phases - germinal vesicle (GV),

This article is part of a special issue entitled: Oogenesis published in *Developmental Biology*.

* Corresponding author. Genetics Unit, Department of Pathology, Faculty of Medicine University of Porto (FMUP), 4200-319, Portugal.

E-mail address: cmarques@med.up.pt (C.J. Marques).

¹ Current address: Altos Labs Cambridge Institute of Science, CB21 6 GP Cambridge, UK.

² Co-senior authors.

<https://doi.org/10.1016/j.ydbio.2024.12.004>

Received 18 November 2024; Accepted 11 December 2024

Available online 15 December 2024

0012-1606/© 2024 The Authors. Published by Elsevier Inc. This is an open access article under the CC BY-NC license (<http://creativecommons.org/licenses/by-nc/4.0/>).

containing an intact nuclear envelope; metaphase I (MI) showing a homogeneous cytoplasm; and metaphase II (MII), after extrusion of the first polar body, which remain arrested until fertilization occurs (Sang et al., 2021).

Oocytes are transcriptionally active during the growth phase, but transcription halts before oocyte maturation, at the prophase-arrested germinal vesicle stage, showing highly condensed chromatin surrounding the nucleolus (Clift and Schuh, 2013; De La Fuente et al., 2004). It is not until after fertilization that transcription fully resumes. It was initially accepted that embryonic genome activation would start between the four- and eight-cell stage in human preimplantation development (Braude et al., 1988) although recent evidence suggests that it initiates at the one-cell stage (Asami et al., 2022). The timing of transcriptional repression in GV oocytes is an important developmental transition to enable oocyte's full developmental potential (De La Fuente et al., 2004). The global silencing of transcription is accomplished due to chromatin modification, such as methylation and deacetylation of histones and DNA methylation (He et al., 2021). Chromatin in the oocyte nucleus changes from a diffuse or decondensed configuration, found predominantly in growing diplotene stage oocytes, and becomes progressively condensed around the nucleolus upon completion of oocyte growth (De La Fuente et al., 2004). Post-transcriptional control of gene expression ensures the storage and timely activation of maternal factors necessary for the oocyte-to-embryo transition. Noteworthy, transcripts are stored during oocyte growth to support oocyte maturation and are subsequently selectively degraded during maturation (Su et al., 2007). Since transcription is postulated to be absent during oocyte maturation, post-transcriptional regulation of mRNAs plays an essential role in the process. Immature oocytes contain transcripts with shorter poly-adenylated tails, which are stored in subcortical aggregates in the cytoplasm, ready for subsequent reactivation (Clift and Schuh, 2013). Following the onset of oocyte maturation, polyadenylation of dormant transcripts occurs in the cytoplasm, activating these mRNAs and enabling them to be translated (Clift and Schuh, 2013; Liu et al., 2023).

Epigenetic modifications play a central role in regulation of gene expression. The histone modifications H3K9 and H3K4 trimethylation are well-characterized epigenetic marks that have been shown to be associated with transcriptional silencing in oocytes (Andreu-Vieyra et al., 2010; Chousal et al., 2018). Besides histone modifications, the oocyte acquires a unique DNA methylation pattern during oocyte growth, in which an increase in global levels of DNA methylation correlates with chromatin accessibility and active transcription (Qian and Guo, 2022). DNA methylation is catalysed by the DNA methyltransferase (DNMT) protein family, which is responsible for adding a methyl group to the fifth carbon of cytosine bases, predominantly in CpG dinucleotides, yielding a 5-methylcytosine (5 mC) (Portela and Esteller, 2010). 5 mC can be oxidized by the action of the ten-eleven translocation (TET) protein family, namely, TET1, TET2, and TET3, resulting in 5-hydroxymethylcytosine (5hmC), which is implicated in the active DNA demethylation mechanism (Branco et al., 2011). In human oocytes, studies using single-cell whole-genome bisulfite sequencing showed no differences in the global CpG methylation between GV to MII stage, although localized changes still occur throughout maturation (Yu et al., 2017). Noteworthy, non-CpG methylation levels increase from GV to MII stages, being associated with gene expression changes during maturation and directed by DNMT3B (Yu et al., 2020). Intriguingly, oocytes present a bimodal pattern of DNA methylation, i.e., methylation is largely restricted to actively transcribed regions, with intergenic or transcriptionally inactive regions showing low levels of methylation (Demond and Kelsey, 2020). Furthermore, transcription and chromatin accessibility correlate with *de novo* DNA methylation in growing oocytes (Yan et al., 2021), with transcription being required for the establishment of DNA methylation at imprinted genes in mouse oocytes (Chotalia et al., 2009).

The study of the oocyte transcriptome during maturation is of great relevance, as gene expression during their growth affects the quality of

the oocytes (Fan et al., 2015). Studies have shown that non-competent oocytes have a different transcriptional state compared to competent oocytes (Yanez et al., 2016). Thus, a comprehensive knowledge of the oocyte transcriptome is important for assisted reproductive technologies (ART), particularly the potential to improve *in vitro* maturation protocols, since it has been observed that *in vitro* matured oocytes express different genes compared to *in vivo* matured oocytes (Jones et al., 2008; Zhao et al., 2019). The transcriptome of oocytes has initially been studied using microarrays (Jones et al., 2008; Kocabas et al., 2006). With the development of Next-Generation Sequencing (NGS) techniques to analyse transcriptomes at a single cell level, it has been possible to study the oocyte transcriptome in several mammalian species (Tang et al., 2010); however, the study in humans is still limited, especially in *in vivo* matured MII oocytes. In this study, we analysed the transcriptome of human oocytes at three different maturation stages, using single-oocyte RNA-Seq, with the aim of providing a transcriptomic profile and identifying key genes driving oocyte maturation.

2. Materials and methods

2.1. Single oocyte collection

Human oocytes analysed in this prospective study were collected from surplus material of oocyte donation programs from Assisted Reproduction Centres in Porto, Portugal (CRGAB - Centre for Reproductive Genetics Professor Alberto Barros and PROCRIAR Fertility Clinic), after obtaining informed consent from the donors. Characterization of all the oocyte donors is presented in [Supplemental Table S1](#), with no statistically significant differences observed regarding Age, Body Mass Index (BMI) or Smoking status. All biological materials were donated voluntarily, anonymously and carried no personal identifiers. A routine genetic analysis of karyotype and the most frequent pathogenic variants for cystic fibrosis, spinal muscular atrophy and fragile-X was performed in all the donors, with the presence of a pathogenic/likely-pathogenic variant being an exclusion criterion. This study was approved by the institutional review board (Ethics Committee for Health of Hospital Sao Joao/Faculty of Medicine of the University of Porto -project reference CE 429–19) and conducted in accordance with the Declaration of Helsinki.

Oocyte donors underwent controlled ovarian hyperstimulation with a gonadotropin-releasing hormone (GnRH) antagonist protocol (0.25 mg, ganirelix, Orgalutran, MSD, Hertfordshire, UK). For stimulation, recombinant follicle-stimulating hormone was used (mostly with rFSH, follitropin alfa, Gonal-F; Merck Serono, Geneva, Switzerland and occasionally with Elonva; Organon, Kloosterstraat, Netherlands). For induction of maturation, a GnRH agonist (0.2 mg, triptorelin, Decapeptyl; Ipsen Pharma Biotech, Signes, France) was administered 36h before ultrasound-guided transvaginal oocyte retrieval.

The size of the follicles was monitored over several days before the follicle puncture, which allowed the optimal time for the puncture to be established ([Supplemental Table 3](#)). Therefore, different sizes of follicles were aspirated in puncture. Oocyte handling was performed in Origio media (Origio, Malöv, Denmark) in a heated airflow (K-system, Kivex Biotec, Denmark; Cooper Surgical, Malöv, Denmark). Denudation was performed enzymatically with Cumalase (Origio) and then mechanically in SPM (Origio) with Handling pipettes (Vitrolife). After denudation, oocytes were placed in a tube with 3 μ L of FERT medium (Origio) and immediately stored at -20°C for a maximum of 2 h. The oocytes are then snap-frozen and incubated at -80°C after adding 2.5 μ L of Buffer RLT (Qiagen).

Human oocytes were classified into three distinct maturation stages, according to their morphological characteristics, namely, the presence of an intact and visually distinct nuclear membrane and prominent nucleolus (Germinal Vesicle – GV), the presence of an extruded first polar body (Metaphase II – MII) and a homogeneous cytoplasm (Metaphase I - MI) ([Fig. 1A](#)). Abnormal-appearing oocytes, with signs of

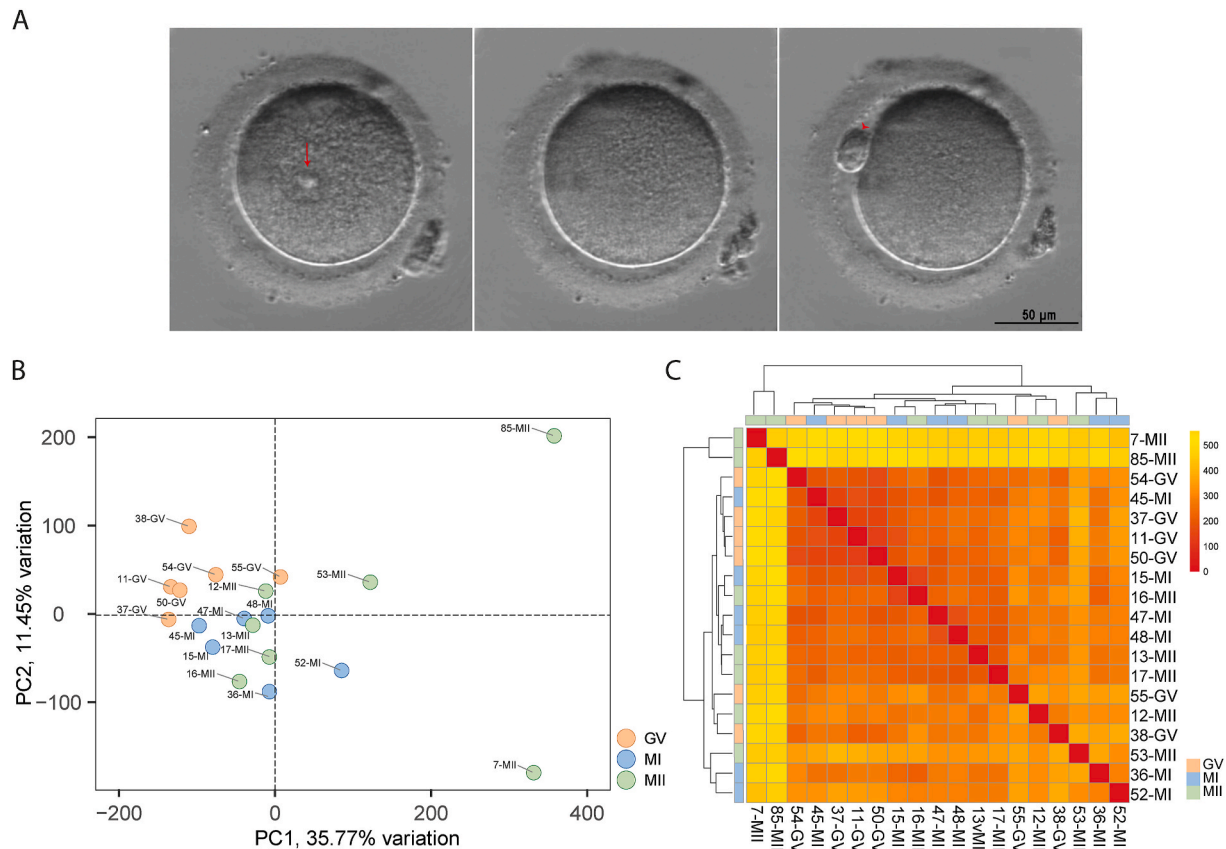


Fig. 1. – Characterization of human oocyte maturation stages. A) Phase-contrast microscopy images of human oocytes at each maturation stage: GV – Germinal-Vesicle; MI – Metaphase I; MII – Metaphase II. Arrow – nuclear envelope in GV oocyte; Arrowhead – first polar body in MII oocyte. B) Principal Component Analysis (PCA) plot of all oocytes. GV oocytes are represented in orange, MI oocyte in blue and MII in green and C) Heatmap showing the correlation coefficients between transcriptomes of all oocytes, reflecting similarities and differences in gene expression across the maturation stages. (For interpretation of the references to color in this figure legend, the reader is referred to the Web version of this article.)

degeneration, were excluded from this study.

2.2. Library preparation for RNA-Seq analysis

To limit the influence of external factors, transcriptome analysis was performed in oocytes collected from a single IVF clinic (CGRAB). A total of 19 oocytes were individually collected, 6 in the Germinal Vesicle stage (Prophase I of the cell cycle; GV), 6 were in Metaphase I (MI) and 7 were in Metaphase II (MII). These oocytes were retrieved from eleven oocyte donors and from only one cycle of ovarian stimulation per donor. Detailed information about the oocytes donors and follicle size before ovarian puncture is provided in [Supplemental Tables S1 and S2](#).

Full-length single-oocyte RNA-seq (soRNA-seq) libraries were prepared at the Genomics Unit of Gulbenkian Institute of Science (IGC, Portugal), following the protocol described by Macaulay and collaborators ([Macaulay et al., 2016](#)). Each single oocyte, collected in RLT reagent (Qiagen), was processed for cDNA synthesis, as described in the original protocol. Quality control of the synthesized cDNA was performed using Fragment Analyzer (Agilent Technologies). Library preparation including cDNA ‘tagmentation’, PCR-mediated adaptor addition and amplification of the adaptor-ligated libraries was performed following the Nextera library preparation protocol (Nextera XT DNA Library Preparation kit, Illumina), as described by Baym and collaborators ([Baym et al., 2015](#)). Amplified libraries were analysed by Fragment Analyzer (Agilent Technologies) and then sequenced in a NextSeq 2000 (Illumina Inc) using 100 SE P2 to an average sequencing depth of 20 million reads per cell. Sequence information was extracted in FastQ format, using Illumina DRAGEN FASTQ Generation v3.8.4.

2.3. Sequencing data processing

Initial quality check of raw sequencing data was performed using FastQC (Babraham BioInformatics) (Version 0.12.0) and was considered of good quality (99% > Q30). Reads were then mapped to the human genome (GRCh38) with Hisat2 v2.2.2 ([Kim et al., 2015](#)). Gene expression quantification was carried out using FeatureCounts (Version 2.0.3) ([Liao et al., 2013](#)) and Kallisto (Version 0.50.0) ([Bray et al., 2016](#)) using gene annotations from Ensembl version 106 (April 2022) in order to compare and validate the results obtained with the two bioinformatic tools. Expression values were normalized to CPM (Counts Per Million) using the Trimmed Mean of the M-Values (TMM) approach ([Robinson and Oshlack, 2010](#)) as available in the edgeR (Version 3.32.1) package from the R software (Version 4.0.5).

2.4. Bioinformatic analysis

Principal component analysis (PCA) was performed with normalized CPM values to assess the overall similarity between samples, using the R package PCAtools (Version 2.2.0). R (Version 4.0.5) was also used to plot a heatmap representing similarity between samples using the Euclidean distance of normalized gene expression.

The expressed genes were determined considering the normalized CPM value, which should be greater than 1 (or log₂CPM greater than 0) in all samples of the group. Genes uniquely expressed in each phase were defined as genes whose normalized CPM value was greater than 1 in all samples from only one of the stages. Differentially Expressed Genes (DEGs) were identified by comparing all oocyte maturation stages (GV vs MI; GV vs MII; MI vs MII). DEGs were identified using the quasi-

likelihood F-test (Lun et al., 2016) as available in the edgeR (Version 3.32.1) package in R (Version 4.0.5). Genes with $FDR \leq 0.05$ and Fold-Change (FC) $> |2|$ were assigned as differentially expressed. As an alternative and less restrictive, tool, DESeq2 (Version 1.30.1) (Love et al., 2014) was also utilized to extract DEGs, using a p adjusted value < 0.05 and $\log_2FC > |1|$.

KEGG pathway (Kyoto Encyclopedia of Genes and Genomes; <http://www.genome.jp/kegg/>) and Gene ontology (GO) analysis (<http://geneontology.org>) was performed using the tool g:GOST provided by GProfiler (Raudvere et al., 2019) (Version e111_eg58_p18_f463989d). GO terms with an adjusted p-value < 0.05 were considered significant. Venn Diagrams were constructed using the VIB/UGent Bioinformatics and Evolutionary Genomics tool - <https://bioinformatics.psb.ugent.be/webtools/Venn/> and jvenn - <https://jvenn.toulouse.inrae.fr/app/index.html> (Bardou et al., 2014).

Volcano plots were plotted to visualize the differentially expressed genes in each comparison using the package EnhancedVolcano (Version 1.8.0) from R. Violin plots were designed using R software and ggplot2 package (Version 3.3.6).

2.5. Gene expression analysis by quantitative RT-PCR (qRT-PCR)

RNA extraction from human oocytes was performed using Power SYBR® Green Cells-to-Ct™ Kit (Invitrogen), allowing reverse transcription (RT) and real-time PCR directly from cell lysates. Briefly, we added 50 μ L of lysis solution (with DNase I) to the single oocyte and incubated at RT for 5 min. Then, 5 μ L of stop solution were added to the lysate and incubated for 2 min at RT. After, 10 μ L of the lysate were used for the reverse transcription reaction and 2 μ L of the cDNA was used for the RT-qPCR, using PowerUp™ SYBR™ Green Master Mix. Gene expression was evaluated using a DNA-binding dye, 2 \times PowerUp SYBR Green Master Mix (Thermo Fisher Scientific), following the manufacturer's instructions. Specific primers were designed for amplification of *DNMT1*, *ZFAND2A* and *UBB* as reference gene (Supplemental Table S4). We analysed the expression of the following genes: *DNMT1* in 9 GV oocytes and 4 MII oocytes, *ZFAND2A* in 10 GV oocytes and 3 MII oocytes. Statistical analysis was performed using the Mann-Whitney *U* test, with the Statistical Package for Social Sciences (SPSS, IBM) software v29.0.

4. Results

4.1. Transcriptome analysis of human oocytes reveals a higher number of expressed and uniquely expressed genes in GV oocytes, comparing to MI and MII oocytes

We isolated single human oocytes that were classified according to their morphological characteristics into three distinct stages: Germinal Vesicle (GV), Metaphase I (MI) and Metaphase II (MII) (Fig. 1A), as described in the Material and Methods section. Then, we performed transcriptomic analysis through single-oocyte RNA-Seq (soRNA-Seq). A total of 19 oocytes, originating from 11 donors, were individually sequenced (6 GV, 6 MI and 7 MII). The number of mapped and aligned reads for each sample is shown in Supplemental Table S3.

Principal component analysis (PCA), after quantification of gene expression using FeatureCounts (Liao et al., 2013), showed relatively dispersed samples but a degree of aggregation based on the oocyte maturation stage was observed, particularly in GV oocytes, which appear predominantly on the upper left quadrant and more distant to the other two stages (Fig. 1B). The group of MI oocytes might include oocytes that are transitioning to MII but have not yet undergone polar body extrusion, hence appearing more closely related to MII oocytes. MII oocytes showed less aggregation in the PCA plot as well as in the distance heatmap (Fig. 1C), which might reflect more heterogeneity of the samples. When using kallisto (Bray et al., 2016) as an alternative tool for gene expression quantification, a PCA plot with the same distribution

was obtained as well as a similar heatmap (Supplementary Figs. S1 and S2).

In order to identify which genes were expressed at each maturation stage, we considered transcripts with a CPM (Counts Per Million) value greater than 1 (or $\log_2CPM > 0$) in all the samples belonging to each group, retrieving a number of expressed genes of 9660 in GV, 8734 in MI and 5889 in MII oocytes (Supplementary File S1). The top 10 most highly expressed genes at each maturation stage are shown in Fig. 2A. Of these, *TUBB8* (Tubulin Beta 8 Class VIII) was the most expressed gene at all maturation stages, along with other genes of the same family (*TUBB8P7* and *TUBB8B*). Mitochondrial genes such as *MT-ND4* and *MT-CO1* were also highly expressed in all maturation stages, as well as the Histone *H3-3B*. Examples of other genes that were highly expressed at all stages were *DPPA3* (Developmental Pluripotency Associated 3), *WEE2* (*WEE2* Oocyte Meiosis Inhibiting Kinase), *OOSP2* (Oocyte Secreted Protein 2), all *ZP* (Zona pellucida) genes, *BMP15* (Bone Morphogenetic Protein 15) and *GDF9* (Growth differentiation factor 9) (Fig. 2A and Supplementary File S1).

Gene ontology analysis of the highly expressed genes ($\log_2CPM > 10$) in each maturation stage revealed similar terms for all three oocyte stages, namely terms related to mitochondrial function and oocyte development and maturation (Supplementary Fig. S3).

Further analysis revealed that, of the genes expressed in each maturation stage, 5602 were common to all three stages whereas 1328 were unique in GV, 401 in MI and 72 in MII (Fig. 2B and Supplementary File S2). GV and MI shared the highest number of genes ($n = 2623$) whereas MI and MII, and GV and MII, shared a similar number of genes ($n = 108$ and 107 , respectively) (Fig. 2B).

Gene Ontology analysis of the 5602 genes that were expressed in all three maturation stages revealed terms related with organelle organization, metabolic and biosynthetic processes as well as cell cycle (Fig. 2C). Regarding molecular function, protein binding was the most significant term, followed by catalytic activity and enzyme binding.

Concerning the uniquely expressed genes and in particular for molecular function, protein binding was the most significant term in GV oocytes followed by catalytic activity, ion binding and transferase activity (Supplemental Table S5). Interestingly, we also obtained the Molecular Function terms “S-adenosylmethionine-dependent methyltransferase activity” and “methyltransferase activity”, possibly related to epigenetic reprogramming events occurring in oocyte development (Qian and Guo, 2022).

Regarding uniquely expressed genes in MI ($n = 401$), we only obtained two statistically significant GO terms which were “biological regulation” and “regulation of biological process” (Supplementary Table S5). No statistically significant GO terms were found for unique genes from MII oocytes, possibly due to the low number of genes analysed.

4.2. Differential expression analysis reveals higher differences between GV and MII maturation stages

In order to identify transcriptomic changes during oocyte maturation, we extracted Differentially Expressed Genes (DEGs) with fold change (FC) $> |2|$ (or $\log_2FC > |1|$) and $FDR < 0.05$ (Supplementary File S3). Using EdgeR (Lun et al., 2016), we identified 42 DEGs between GV and MI and 1165 DEGs between GV and MII stages; no DEGs were detected between MI and MII maturation stages. On the other hand, using DESeq2 (Love et al., 2014) as an alternative method to extract DEGs, we obtained 403 DEGs between GV and MI, 2981 DEGs between GV and MII and 80 DEGs between MI and MII, with a p adjusted value < 0.05 and $\log_2FC > |1|$. Comparison of all the bioinformatic tools utilized revealed EdgeR to be a more stringent tool, capturing less DEGs than DESeq2. Importantly, nearly all EdgeR DEGs were also present in DESeq2 analysis (Supplementary Fig. S4); hence, we proceeded further analyses with the DEGs obtained by EdgeR.

Of the 42 DEGs detected between GV and MI stages, 38 were

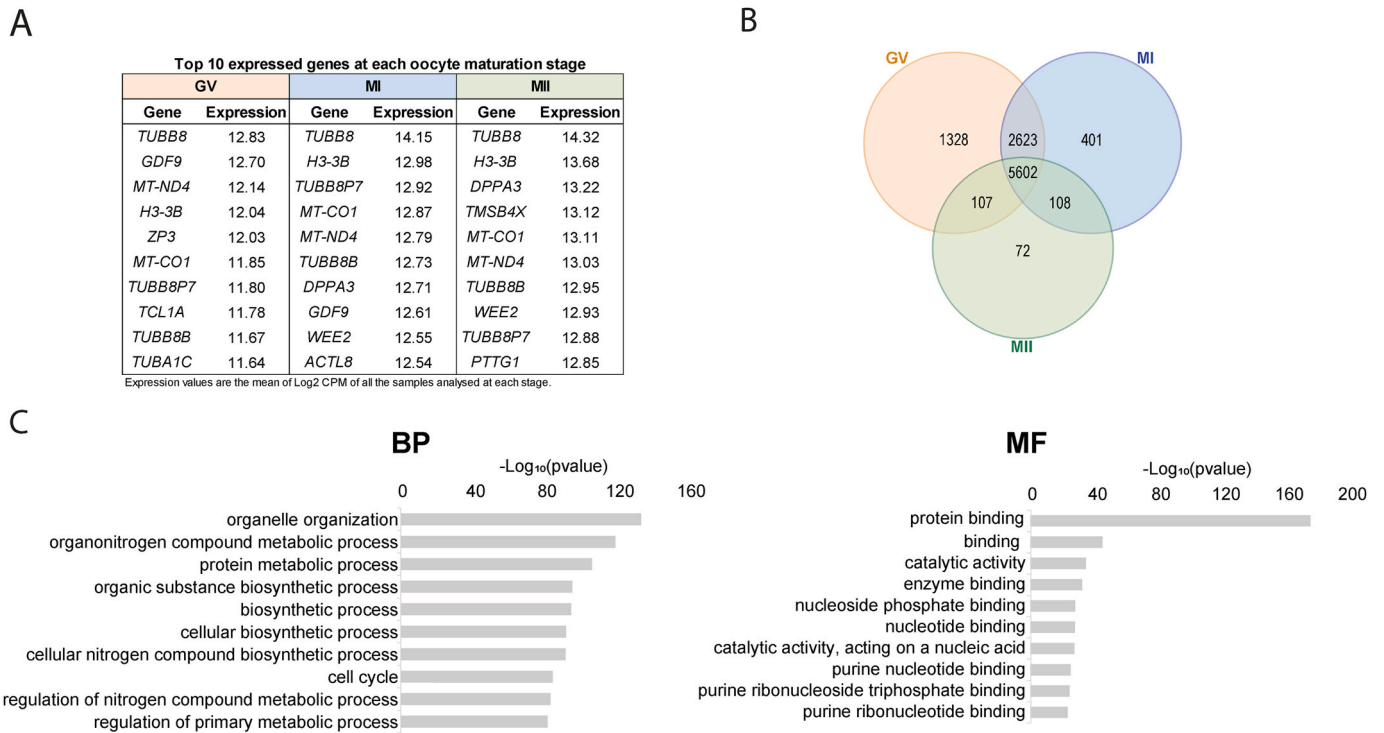


Fig. 2. – Gene expression analysis from the transcriptome. A) Ten most expressed genes at each maturation stage (expression values are the mean value of Log₂CPM of each stage of maturation); B) Venn Diagram showing the number of unique and shared genes in each oocyte maturation stage; C) Gene Ontology (GO) analysis of the 5602 genes commonly expressed in all maturation stages, highlighting the most significant terms associated with biological processes (BP) and molecular functions (MF). GV – Germinal-Vesicle (Prophase I); MI – Metaphase I; MII – Metaphase II. Gene Ontology biological processes (BP) and molecular function (MF) terms.

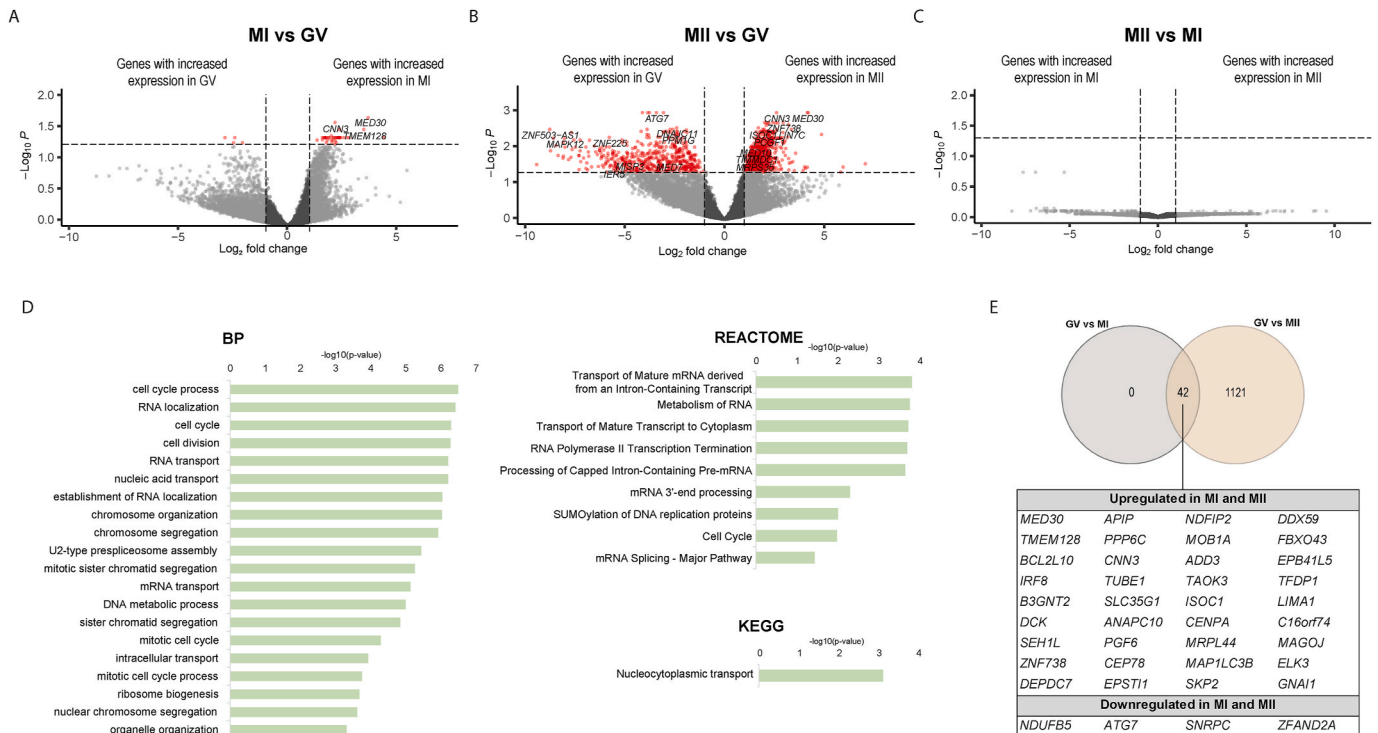


Fig. 3. – Differentially Expressed Genes during oocyte maturation. DEGs were defined as FDR ≤ 0.05 and FoldChange (FC) > |2|. Volcano Plots for comparison between A) MI and GV oocytes B) MII and GV oocytes C) MII and MI oocytes. D) Functional enrichment analysis, displaying the significant Gene Ontology (GO) biological processes (BP), REACTOME pathways, and KEGG pathways associated with upregulated DEGs in MII relative to GV oocytes. E) Venn diagram of DEGs obtained from the comparisons between MI vs. GV and MII vs. GV, showing the overlap and specific DEGs. GV – Germinal-Vesicle; MI – Metaphase I; MII – Metaphase II.

upregulated in MI oocytes and 4 were downregulated (Fig. 3A and Supplementary File S3). GO analysis of the MI upregulated genes revealed an enrichment of the term “mitotic cell cycle” (Supplementary File S3).

Regarding the comparison between GV and MII oocytes, we identified a total of 1165 DEGs, of which 635 were upregulated and 528 were downregulated in MII oocytes (Fig. 3B and Supplementary File S3). GO analysis of the upregulated genes in MII revealed relation to cell cycle processes, RNA localization and transport, chromosome organization and segregation (Fig. 3D and Supplementary File S3). Downregulated genes were related to nucleoplasm and proteasome activity (Supplemental File S3). Noteworthy, all the 42 DEGs identified in the GV vs MI comparison were also present in the GV vs MII comparison, whereas 1121 DEGs were unique to the GV vs MII comparison (Fig. 3E).

Interestingly, no DEGs were identified between MI and MII oocytes, reflecting a similar transcriptional state between oocytes in these two meiotic divisions (Fig. 3C).

Expression plots of some of the DEGs are shown in Fig. 4; *WEE2* and *DPPA3*, two of the top10 highly expressed genes (Fig. 2A), are upregulated throughout oocyte maturation, as well as *CDC20*, which encodes a protein that is a co-activator subunit of anaphase-promoting complex/cyclosome (APC/C) and is crucial for oocyte maturation (Sang et al., 2021).

Examples of downregulated genes are *PANX1* and *PATL2*, which have been implicated in oocyte death and GV arrest, respectively (Sang et al., 2021). *PANX1* encodes pannexin 1, a glycoprotein that has an important role in cellular communication, namely for the transport of adenosine 5'-triphosphate (ATP). Variants in *PANX1* may lead to aberrant ATP release followed by oocyte death (Wang et al., 2021). *PATL2* is an RNA-binding protein that may play the role of translational repressor and biallelic mutations in *PATL2* may lead to oocyte GV arrest, and, therefore, women's infertility (Chen et al., 2017). Another important gene which is also downregulated throughout oocyte maturation is the *ZAR1* (Zygote Arrest 1), in particular for coordination of maternal mRNAs storage, translation and degradation (Rong et al., 2019).

MED30, *ZFAND2A* and *ZNF738* are three of the most significant DEGs, with *MED30* and *ZNF738* being upregulated and *ZFAND2A* being downregulated in MII (confirmed by qRT-PCR in an independent set of samples; Suppl Fig. S5).

4.3. Expression of epigenetic regulators throughout human oocyte maturation

Epigenetic modifications play a pivotal role during oocyte meiotic maturation. Hence, we focused our analysis on the expression of several epigenetic regulators (Fig. 5 and Supplemental File S4). Histone

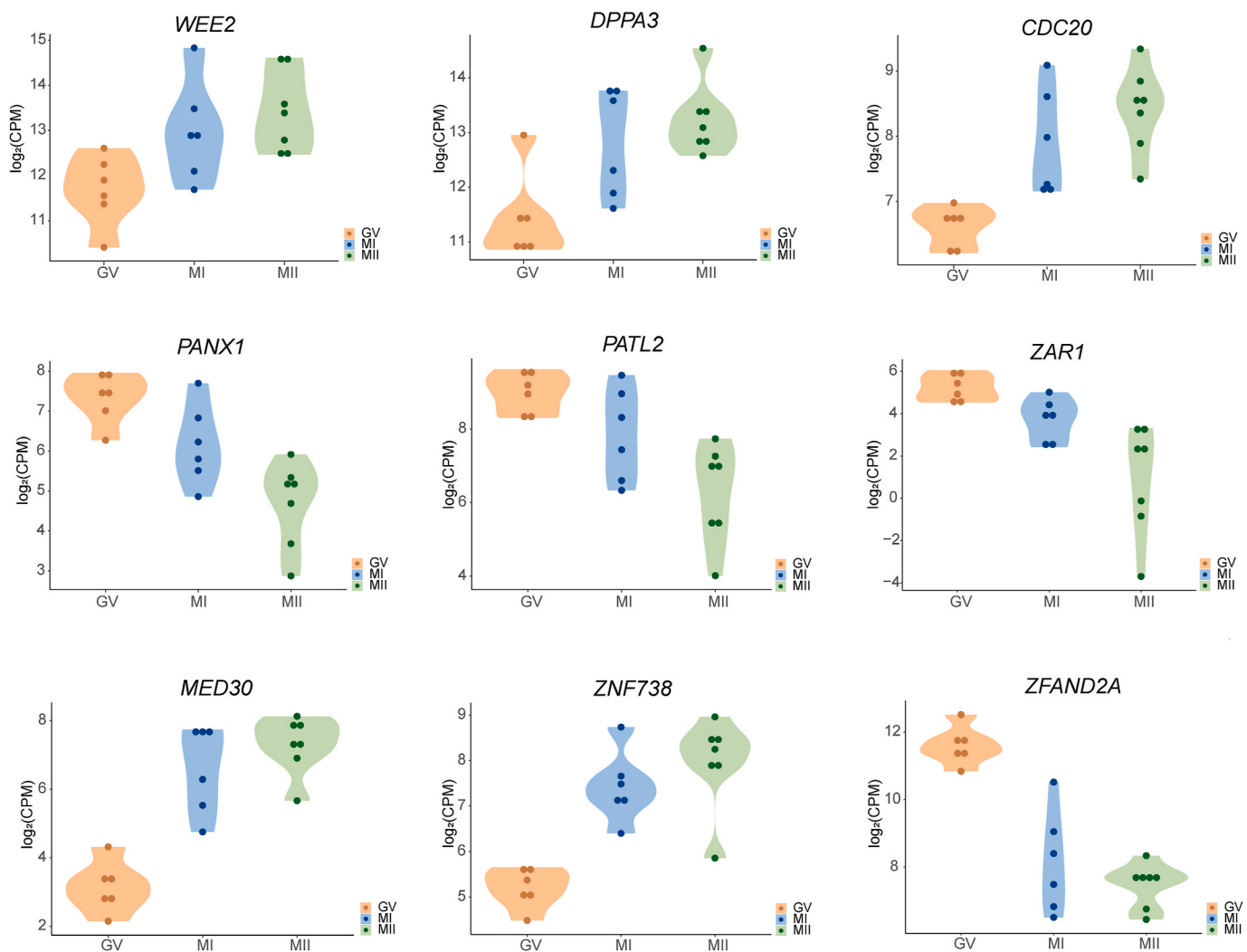


Fig. 4. – Violin plots of Differentially Expressed Genes (DEGs) during oocyte maturation. Violin plots illustrate the expression levels of selected DEGs with $FDR \leq 0.05$ and absolute Fold Change ($FC > |2|$), specifically for the genes: *WEE2*, *DPPA3*, *CDC20*, *PANX1*, *PATL2*, *ZAR1*, *MED30*, *ZNF738* and *ZFAND2A*. Orange: GV oocytes, Blue: MI oocytes, Green: MII oocytes. (For interpretation of the references to color in this figure legend, the reader is referred to the Web version of this article.)

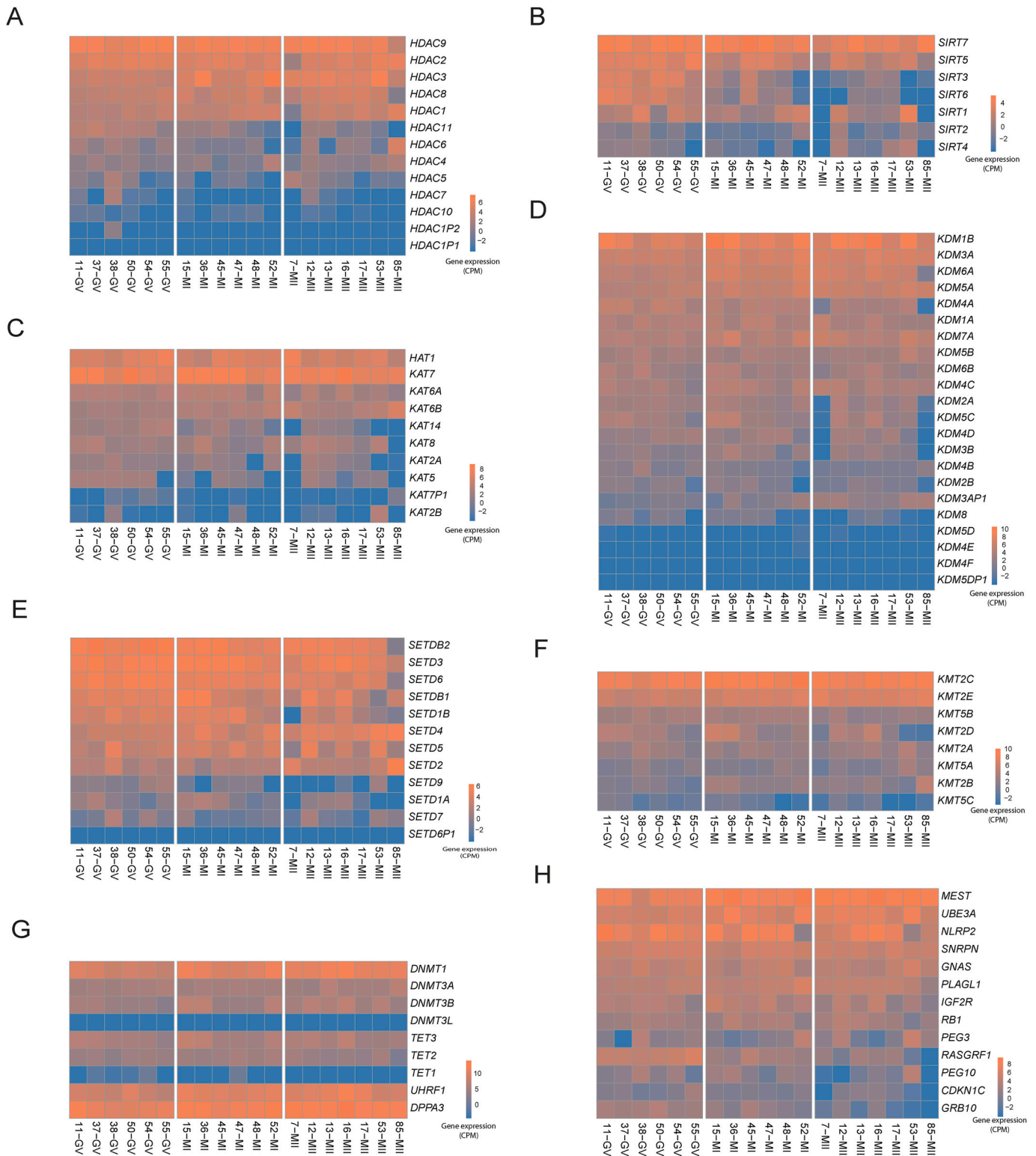


Fig. 5. Heatmaps of epigenetic regulators and imprinted genes. Histone deacetylases (A) and Sirtuins (B); Histone acetyltransferases (C); Histone demethylases (D); SET-domain protein methyltransferases (E); Histone Methyltransferases (F); DNA methyltransferases and co-factors and Demethylases (G); Imprinted genes (H). The color gradient represents the level of gene expression (in CPM). (For interpretation of the references to color in this figure legend, the reader is referred to the Web version of this article.)

deacetylases (HDACs), especially *HDAC9*, *HDAC2* and *HDAC3* were highly expressed in all oocyte maturation stages (Fig. 5A). Sirtuins (SIRT) are nicotinic adenine dinucleotide (+)-dependent histone deacetylases (Wu et al., 2022). Whereas the most expressed Sirtuins throughout all the maturation stages were *SIRT7* and *SIRT5* (Fig. 5B),

SIRT3 and *SIRT6* showed differential expression, being downregulated in MII oocytes (Supplemental File S3).

Regarding histone acetyltransferases, *HAT1* and *KAT7* were the most highly expressed throughout meiotic maturation (Fig. 5C). Other histone-modifying enzymes that were highly expressed in all stages were

lysine demethylases (KDM), particularly *KDM1B* and *KDM3A* (Fig. 5D). Of all the KDMs, only *KDM3AP1* was identified as a DEG showing increased expression in MII oocytes (Supplemental File S3).

When we examined histone methyltransferase enzymes, such as the SET domain (SETD) and histone lysine methyltransferase (KMT), we observed that, in general, *SETD* exhibited higher expression levels in the three maturation stages (Fig. 5E). However, it was the *KMT2C* gene that showed the highest expression (Fig. 5F). Additionally, of all the histone methyltransferases, only *KMT2E* was identified as a DEG, showing upregulation in MII oocytes (Supplemental File S3).

Regarding DNA methylation writers, *DNMT1* (DNA methyltransferase 1) showed high expression during oocyte maturation and upregulation in MII oocytes (confirmed by qRT-PCR in an independent set of samples; Suppl Fig. S5), together with its recruiter *UHRF1* and binder *DPPA3* (Fig. 5G). Of the TET-family of enzymes, which play a role in the active DNA demethylation process, *TET3* was the most highly expressed, consistent with previous observations in the mouse oocyte and its role in the conversion of 5 mC to 5hmC in the early zygote (Wossidlo et al., 2011). Regarding imprinted genes, we observed a high expression of mesoderm-specific transcript (*MEST*), Ubiquitin Protein Ligase E3A (*UBE3A*) and NLR Family Pyrin Domain Containing 2 (*NLRP2*) genes in all stages of oocyte maturation (Fig. 5H). Additionally, we observed that *MEST* was upregulated in MII oocytes whereas Ras Protein Specific Guanine Nucleotide Releasing Factor 1 (*RASGRF1*) was downregulated (Supplemental File S3).

5. Discussion

In this study, we performed transcriptomic analysis of human oocytes in three developmental stages of the meiotic maturation process. The quality of oocytes and embryos in the IVF lab is determined by morphological markers, whereas there is a lack of molecular markers for determining oocyte quality (Sang et al., 2021). Our results describe the gene expression patterns in each stage of oocyte maturation, with the number of genes expressed showing a reduction from GV to MI and subsequently from MI to MII, which is consistent with RNA degradation observed during oocyte maturation (Jiang and Fan, 2022). This decrease in the number of expressed genes during oocyte maturation has been documented by other authors (Llonch et al., 2021; Takeuchi et al., 2022; Yan et al., 2021; Yu et al., 2020). Indeed, in a recent meta-analysis including human oocyte transcriptomic data from 6 independent studies, a 30% decline in total mRNA from GV to MII stage was described (Ducreux et al., 2023). Interestingly, we found that the number of unique genes, i.e., genes that were only expressed in one of the oocyte stages, also decreased from GV to MII, as observed by others (Yu et al., 2020), albeit the number of unique genes we observed is substantially higher than the number reported by Yu and collaborators. Furthermore, in our study, 72 genes are uniquely expressed in MII stage, and 635 genes are upregulated during oocyte maturation, from GV to MII stages, reinforcing the idea that transcriptional regulation occurs throughout meiotic divisions. As proposed by Ducreux and colleagues, this may reflect the amount of mRNAs that can be recruited for translation and therefore have not been targeted for degradation due to shorter polyA tails. It could also result from polyA tail lengthening during the GV to MII transition, leading to their upregulation in MII oocytes (Ducreux et al., 2023).

We obtained a high number of differentially expressed genes when comparing GV and MII oocytes, some of which are known to be relevant for oocyte maturation. In fact, of these DEGs, 148 were also observed by Pietroforte and collaborators (Pietroforte et al., 2023), of which we highlight some that were deemed to be relevant for the maturation of the oocyte, such as the *ZAR1*, *PATL2*, *TRIP13*, *RBBP7* and *WEE2*. Additionally, *ZAR1*, *PATL2*, *RBBP7* and *WEE2* were also identified as differentially expressed genes by Yu and collaborators, between MII oocytes and MI oocytes (Yu et al., 2020), highlighting the robustness of the results across different laboratories and studied populations.

Regarding the expression of specific genes, *TUBB8* was the most highly expressed gene across all three stages. *TUBB8* encodes a primary beta-tubulin subunit of oocytes and early embryos and has a key role in meiotic spindle assembly and maturation in human oocytes; it has been shown that mutations in *TUBB8* result in maturation arrest at meiosis I, by disrupting microtubule behaviour and oocyte spindle assembly, leading to female infertility (Feng et al., 2016). *TUBB8B* and *TUBB8P7* were also highly expressed in all three stages; *TUBB8B* is a paralog of *TUBB8* and a protein coding gene whereas *TUBB8P7* is a pseudogene. Several mitochondrial genes were also highly expressed in all maturation stages, consistent with the reported abundance of mitochondria in oocytes; *MT-ND4* and *MT-CO1* were the most highly expressed. Another gene that was also observed to be highly expressed was the gene *H3-3B* that codes for histone variant H3.3, which was shown to be essential for paternal chromatin remodelling after fertilization and for the subsequent paternal genome activation during embryogenesis (Kong et al., 2018). Other highly expressed genes of note are *DPPA3* (a.k.a. STELLA), which is essential for female fertility and encodes a protein that plays an important role in shaping the oocyte methylome, preventing *de novo* methylation by UHRF1-mediated DNMT1 (Li et al., 2018). Additionally, *WEE2* and *OOSP2*, are critical for meiosis and, therefore, for oocyte maturation (Hu et al., 2022; Sang et al., 2018). *BMP15* and *GDF9* encode for two oocyte-derived factors that regulate granulosa cell proliferation and differentiation and induce antrum formation (Alam and Miyano, 2020).

Regarding the differential expression throughout oocyte maturation, we observed that genes involved in cell cycle, RNA processes and epigenetic regulation were upregulated in MII oocytes, as noted by Ducreux and collaborators (Ducreux et al., 2023) whereas, in our study, the MII downregulated genes were related to proteasome complex, indicating that maternal protein degradation occurs predominantly before MII stage, being inhibited or halted during the MII oocyte arrest (Karabinova et al., 2011).

Interestingly, *DNMT1*, which is considered a maintenance DNA methyltransferase, i.e., copying with high fidelity the methylation patterns during DNA replication in the S-phase of the cell cycle, is highly expressed throughout oocyte maturation, including across meiotic divisions, being significantly upregulated in MII oocytes, as observed by others (Yu et al., 2020). We have previously observed high expression of *DNMT1* also during meiotic divisions of human spermatogenic cells (Marques et al., 2011), suggesting that DNMT1 might play a role in methylation repair to prevent methylation errors, particularly at imprinted genes, to be transmitted to the next generation. Indeed, DNMT1 has been suggested to act as a *de novo* methyltransferase upon its discovery (Yoder et al., 1997) and later shown to be regulated by *DPPA3* (a.k.a. Stella), safeguarding the unique oocyte epigenome (Li et al., 2018). *UHRF1* (a.k.a. NP95), which is believed to recruit *DNMT1* (Sharif et al., 2007), also had a high expression in all oocyte maturation stages.

Concerning DNA demethylation, two of the putative DNA demethylases, *TET2* and *TET3*, were also expressed in all oocyte maturation stages; in particular, *TET3* has been shown to be highly expressed in mouse oocytes and act upon the active DNA demethylation events observed in the paternal pronucleus of mouse zygotes (Gu et al., 2011; Wossidlo et al., 2011).

We consider that a strength of our work is that we performed transcriptomic analysis in single oocytes given that single-cell RNA sequencing can identify differences which were previously overlooked with bulk analysis (Wu, 2022); additionally, we analysed MII oocytes that underwent *in vivo* maturation, whereas several other studies performed *in vitro* maturation; furthermore, considering that each fertility clinic relies on their own gonadotropin stimulation protocol, another advantage of our study is that transcriptomic analysis was performed in human oocytes collected from a single fertility clinic. Concerning limitations, one possible shortcoming is that we utilized an oligo-dT primer for RNA capture and cDNA synthesis (Macaulay et al., 2016) which directs the transcriptome towards poly-A-tailed mRNAs. Nevertheless,

RNA-Seq protocols that capture only polyadenylated mRNAs have been utilized by other authors to analyse the human oocyte transcriptome (Llonch et al., 2021; Ntostis et al., 2021; Reyes et al., 2017; Takeuchi et al., 2022; Yu et al., 2020). As oocytes are postulated to be transcriptionally silent, changes in gene expression during maturation might be controlled by post-transcriptional mechanisms, such as cytoplasmic polyadenylation of stored mRNAs. mRNA Poly(A) tails, which promote translation and prevent degradation, undergo size changes throughout oocyte maturation, whereas proteins highly important for meiotic divisions have increased polyadenylation during maturation (Liu et al., 2023; Yang et al., 2020).

In conclusion, our study provides novel insights about gene expression changes specific to oocyte maturation, namely a marked reduction in the overall number of expressed genes from GV to MII stage, with a higher number of genes specifically expressed in MII stage oocytes. We also underscore a high expression of DNMT1 through maturation. We noted high expression of several mitochondrial genes, as well as, TUBB8 gene, a critical gene for meiotic spindle assembly, across all stages. Finally, our results show that genes involved in cell cycle regulation, RNA processing, and epigenetic control are significantly upregulated at the MII stage, while proteasome-related genes are downregulated, suggesting a shift in maternal protein degradation timing. Together, these findings expand our understanding of the molecular mechanisms underlying oocyte quality and maturation, contributing for greater understanding of oocyte quality and improvement of fertility treatments.

CRedit authorship contribution statement

Carla Caniçais: Investigation, Methodology, Visualization, Writing – original draft. **Daniel Sobral:** Data curation, Formal analysis, Software, Validation, Writing – review & editing. **Sara Vasconcelos:** Data curation, Formal analysis, Investigation, Methodology, Writing – original draft. **Mariana Cunha:** Investigation, Methodology, Writing – original draft. **Alice Pinto:** Investigation, Methodology, Writing – original draft. **Joana Mesquita Guimarães:** Investigation, Methodology, Supervision, Writing – original draft. **Fátima Santos:** Formal analysis, Investigation, Methodology, Supervision, Visualization, Writing – original draft. **Alberto Barros:** Conceptualization, Formal analysis, Funding acquisition, Investigation, Methodology, Supervision, Validation, Visualization, Writing – original draft. **Sofia Dória:** Conceptualization, Formal analysis, Funding acquisition, Investigation, Methodology, Project administration, Supervision, Validation, Visualization, Writing – original draft, Writing – review & editing. **C. Joana Marques:** Conceptualization, Data curation, Formal analysis, Funding acquisition, Investigation, Methodology, Supervision, Validation, Visualization, Writing – original draft, Writing – review & editing.

Data availability

The datasets and codes generated in this study were deposited in Zenodo (<https://doi.org/10.5281/zenodo.14163312>). All the other data are available from the corresponding author upon reasonable request.

Funding

This work was funded by Fundação para a Ciência e a Tecnologia (FCT, Portugal) - through doctoral fellowships to C.C. (SFRH/141855/2018) and S.V. (SFRH/BD/147,440/2019), a researcher contract to C.J.M. (CEECIND/00371/2017) and a research project grant (EXPL/MED-GEN/1261/2021).

Declaration of competing interest

The authors declare that they have no conflict of interest.

Acknowledgements

We thank all lab members for their support and helpful discussions. We also acknowledge the laboratory embryologists of CGRAB and PROCRIAR fertility clinics for help with collection of the samples and João Sobral, Susana Landeiro and Cathy Paulino (IGC – Instituto Gulbenkian de Ciência, Oeiras, Portugal) for technical assistance with the oocyte single-cell RNA-Seq. Lastly, we would like to thank all the oocyte donors for consenting that surplus material would be used for this research project.

Appendix A. Supplementary data

Supplementary data to this article can be found online at <https://doi.org/10.1016/j.ydbio.2024.12.004>.

References

- Alam, M.H., Miyano, T., 2020. Interaction between growing oocytes and granulosa cells in vitro. *Reprod. Med. Biol.* 19, 13–23.
- Andreu-Vieyra, C.V., Chen, R., Agno, J.E., Glaser, S., Anastassiadis, K., Stewart, A.F., Matzuk, M.M., 2010. MLL2 is required in oocytes for bulk histone 3 lysine 4 trimethylation and transcriptional silencing. *PLoS Biol.* 8, e1000453.
- Asami, M., Lam, B.Y.H., Ma, M.K., Rainbow, K., Braun, S., VerMilyea, M.D., Yeo, G.S.H., Perry, A.C.F., 2022. Human embryonic genome activation initiates at the one-cell stage. *Cell Stem Cell* 29, 209–216.
- Bardou, P., Mariette, J., Escudie, F., Djemiel, C., Klopp, C., 2014. jvenn: an interactive Venn diagram viewer. *BMC Bioinf.* 15, 293.
- Baym, M., Kryazhimskiy, S., Lieberman, T.D., Chung, H., Desai, M.M., Kishony, R., 2015. Inexpensive multiplexed library preparation for megabase-sized genomes. *PLoS One* 10, e0128036.
- Branco, M.R., Ficz, G., Reik, W., 2011. Uncovering the role of 5-hydroxymethylcytosine in the epigenome. *Nat. Rev. Genet.* 13, 7–13.
- Braude, P., Bolton, V., Moore, S., 1988. Human gene expression first occurs between the four- and eight-cell stages of preimplantation development. *Nature* 332, 459–461.
- Bray, N.L., Pimentel, H., Melsted, P., Pachter, L., 2016. Near-optimal probabilistic RNA-seq quantification. *Nat. Biotechnol.* 34, 525–527.
- Chen, B., Zhang, Z., Sun, X., Kuang, Y., Mao, X., Wang, X., Yan, Z., Li, B., Xu, Y., Yu, M., Fu, J., Mu, J., Zhou, Z., Li, Q., Jin, L., He, L., Sang, Q., Wang, L., 2017. Biallelic mutations in PATL2 cause female infertility characterized by oocyte maturation arrest. *Am. J. Hum. Genet.* 101, 609–615.
- Chotalia, M., Smallwood, S.A., Ruf, N., Dawson, C., Lucifero, D., Frontera, M., James, K., Dean, W., Kelsey, G., 2009. Transcription is required for establishment of germline methylation marks at imprinted genes. *Genes Dev.* 23, 105–117.
- Chousal, J.N., Cho, K., Ramaiah, M., Skarbræk, D., Mora-Castilla, S., Stumpo, D.J., Lykke-Andersen, J., Laurent, L.C., Blackshear, P.J., Wilkinson, M.F., Cook-Andersen, H., 2018. Chromatin modification and global transcriptional silencing in the oocyte mediated by the mRNA decay activator ZFP36L2. *Dev. Cell* 44, 392–402. e397.
- Clift, D., Schuh, M., 2013. Restarting life: fertilization and the transition from meiosis to mitosis. *Nat. Rev. Mol. Cell Biol.* 14, 549–562.
- De La Fuente, R., Viveiros, M.M., Burns, K.H., Adashi, E.Y., Matzuk, M.M., Jj, Eppig, 2004. Major chromatin remodeling in the germinal vesicle (GV) of mammalian oocytes is dispensable for global transcriptional silencing but required for centromeric heterochromatin function. *Dev. Biol.* 275, 447–458.
- Demond, H., Kelsey, G., 2020. The enigma of DNA methylation in the mammalian oocyte. *F1000Res* 9.
- Ducreux, B., Ferreux, L., Patrat, C., Fauque, P., 2023. Overview of gene expression dynamics during human oogenesis/folliculogenesis. *Int. J. Mol. Sci.* 25.
- Eppig, J.J., O'Brien, M., Wigglesworth, K., 1996. Mammalian oocyte growth and development in vitro. *Mol. Reprod. Dev.* 44, 260–273.
- Fan, Y., Zhao, H.-C., Liu, J., Tan, T., Ding, T., Li, R., Zhao, Y., Yan, J., Sun, X., Yu, Y., Qiao, J., 2015. Aberrant expression of maternal Plk1 and Dctn3 results in the developmental failure of human in-vivo- and in-vitro-matured oocytes. *Sci. Rep.* 5, 8192.
- Feng, R., Sang, Q., Kuang, Y., Sun, X., Yan, Z., Zhang, S., Shi, J., Tian, G., Luchniak, A., Fukuda, Y., Li, B., Yu, M., Chen, J., Xu, Y., Guo, L., Qu, R., Wang, X., Sun, Z., Liu, M., Shi, H., Wang, H., Feng, Y., Shao, R., Chai, R., Li, Q., Xing, Q., Zhang, R., Nogales, E., Jin, L., He, L., Gupta Jr., M.L., Cowan, N.J., Wang, L., 2016. Mutations in TUBB8 and human oocyte meiotic arrest. *N. Engl. J. Med.* 374, 223–232.
- Gu, T.P., Guo, F., Yang, H., Wu, H.P., Xu, G.F., Liu, W., Xie, Z.G., Shi, L., He, X., Jin, S.G., Iqbal, K., Shi, Y.G., Deng, Z., Szabo, P.E., Pfeifer, G.P., Li, J., Xu, G.L., 2011. The role of Tet3 DNA dioxygenase in epigenetic reprogramming by oocytes. *Nature* 477, 606–610.
- He, M., Zhang, T., Yang, Y., Wang, C., 2021. Mechanisms of oocyte maturation and related epigenetic regulation. *Front. Cell Dev. Biol.* 9, 654028.
- Hu, W., Zeng, H., Shi, Y., Zhou, C., Huang, J., Jia, L., Xu, S., Feng, X., Zeng, Y., Xiong, T., Huang, W., Sun, P., Chang, Y., Li, T., Fang, C., Wu, K., Cai, L., Ni, W., Li, Y., Yang, Z., Zhang, Q.C., Chian, R., Chen, Z., Liang, X., Kee, K., 2022. Single-cell transcriptome and translome dual-omics reveals potential mechanisms of human oocyte maturation. *Nat. Commun.* 13.

- Jiang, Z.Y., Fan, H.Y., 2022. Five questions toward mRNA degradation in oocytes and preimplantation embryos: when, who, to whom, how, and why? *Biol. Reprod.* 107, 62–75.
- Jones, G.M., Cram, D.S., Song, B., Magli, M.C., Gianaroli, L., Lacham-Kaplan, O., Findlay, J.K., Jenkin, G., Trounson, A.O., 2008. Gene expression profiling of human oocytes following *in vivo* or *in vitro* maturation. *Hum. Reprod.* 23, 1138–1144.
- Karabinova, P., Kubelka, M., Susor, A., 2011. Proteasomal degradation of ubiquitinated proteins in oocyte meiosis and fertilization in mammals. *Cell Tissue Res.* 346, 1–9.
- Kim, D., Langmead, B., Salzberg, S.L., 2015. HISAT: a fast spliced aligner with low memory requirements. *Nat. Methods* 12, 357–360.
- Kocabas, A.M., Crosby, J., Ross, P.J., Otu, H.H., Beyhan, Z., Can, H., Tam, W.-L., Rosa, G. J.M., Halgren, R.G., Lim, B., Fernandez, E., Cibelli, J.B., 2006. The transcriptome of human oocytes. *Proc. Natl. Acad. Sci. USA* 103, 14027–14032.
- Kong, Q., Banaszynski, L.A., Geng, F., Zhang, X., Zhang, J., Zhang, H., O'Neill, C.L., Yan, P., Liu, Z., Shido, K., Palermo, G.D., Allis, C.D., Rafii, S., Rosenwaks, Z., Wen, D., 2018. Histone variant H3.3-mediated chromatin remodeling is essential for paternal genome activation in mouse preimplantation embryos. *J. Biol. Chem.* 293, 3829–3838.
- Li, Y., Zhang, Z., Chen, J., Liu, W., Lai, W., Liu, B., Li, X., Liu, L., Xu, S., Dong, Q., Wang, M., Duan, X., Tan, J., Zheng, Y., Zhang, P., Fan, G., Wong, J., Xu, G.-L., Wang, Z., Wang, H., Gao, S., Zhu, B., 2018. Stella safeguards the oocyte methylome by preventing de novo methylation mediated by DNMT1. *Nature* 564, 136–140.
- Liao, Y., Smyth, G.K., Shi, W., 2013. featureCounts: an efficient general purpose program for assigning sequence reads to genomic features. *Bioinformatics* 30, 923–930.
- Liu, Y., Zhao, H., Shao, F., Zhang, Y., Nie, H., Zhang, J., Li, C., Hou, Z., Chen, Z.-J., Wang, J., Zhou, B., Wu, K., Lu, F., 2023. Remodeling of maternal mRNA through poly(A) tail orchestrates human oocyte-to-embryo transition. *Nat. Struct. Mol. Biol.* 30, 200–215.
- Llonch, S., Barragán, M., Nieto, P., Mallol, A., Elosua-Bayes, M., Lorden, P., Ruiz, S., Zambelli, F., Heyn, H., Vassena, R., Payer, B., 2021. Single human oocyte transcriptome analysis reveals distinct maturation stage-dependent pathways impacted by age. *Aging Cell* 20.
- Love, M.I., Huber, W., Anders, S., 2014. Moderated estimation of fold change and dispersion for RNA-seq data with DESeq2. *Genome Biol.* 15, 550.
- Lun, A.T., Chen, Y., Smyth, G.K., 2016. It's DE-licious: a recipe for differential expression analyses of RNA-seq experiments using quasi-likelihood methods in edgeR. *Methods Mol. Biol.* 1418, 391–416.
- Macaulay, L.C., Teng, M.J., Haerty, W., Kumar, P., Ponting, C.P., Voet, T., 2016. Separation and parallel sequencing of the genomes and transcriptomes of single cells using G& T-seq. *Nat. Protoc.* 11, 2081–2103.
- Marques, C.J., Pinho, M. João, Carvalho, F., Bièche, I., Barros, A., Sousa, M., 2011. DNA methylation imprinting marks and DNA methyltransferase expression in human spermatogenic cell stages. *Epigenetics* 6, 1354–1361.
- Ntostis, P., Iles, D., Kokkali, G., Vaxevanoglou, T., Kanavakis, E., Pantou, A., Huntriss, J., Pantos, K., Picton, H.M., 2021. The impact of maternal age on gene expression during the GV to MII transition in euploid human oocytes. *Hum. Reprod.* 37, 80–92.
- Pietroforte, S., Barragan Monasterio, M., Ferrer-Vaquero, A., Irimia, M., Ibáñez, E., Popovic, M., Vassena, R., Zambelli, F., 2023. Specific processing of meiosis-related transcript is linked to final maturation in human oocytes. *Mol. Hum. Reprod.* 29.
- Portela, A., Esteller, M., 2010. Epigenetic modifications and human disease. *Nat. Biotechnol.* 28, 1057–1068.
- Qian, J., Guo, F., 2022. De novo programming: establishment of epigenome in mammalian oocytes. *Biol. Reprod.* 107, 40–53.
- Raudvere, U., Kolberg, L., Kuzmin, I., Arak, T., Adler, P., Peterson, H., Vilo, J., 2019. g:Profiler: a web server for functional enrichment analysis and conversions of gene lists. *Nucleic Acids Res.* 47, W191–w198.
- Reyes, J.M., Silva, E., Chitwood, J.L., Schoolcraft, W.B., Krisher, R.L., Ross, P.J., 2017. Differing molecular response of young and advanced maternal age human oocytes to IVF. *Hum. Reprod.* 32, 2199–2208.
- Robinson, M.D., Oshlack, A., 2010. A scaling normalization method for differential expression analysis of RNA-seq data. *Genome Biol.* 11, R25.
- Rong, Y., Ji, S.-Y., Zhu, Y.-Z., Wu, Y.-W., Shen, L., Fan, H.-Y., 2019. ZAR1 and ZAR2 are required for oocyte meiotic maturation by regulating the maternal transcriptome and mRNA translational activation. *Nucleic Acids Res.* 47, 11387–11402.
- Sang, Q., Li, B., Kuang, Y., Wang, X., Zhang, Z., Chen, B., Wu, L., Lyu, Q., Fu, Y., Yan, Z., Mao, X., Xu, Y., Mu, J., Li, Q., Jin, L., He, L., Wang, L., 2018. Homozygous mutations in WEE2 cause fertilization failure and female infertility. *Am. J. Hum. Genet.* 102, 649–657.
- Sang, Q., Zhou, Z., Mu, J., Wang, L., 2021. Genetic factors as potential molecular markers of human oocyte and embryo quality. *J. Assist. Reprod. Genet.* 38, 993–1002.
- Sharif, J., Muto, M., Takebayashi, S., Suetake, I., Iwamatsu, A., Endo, T.A., Shinga, J., Mizutani-Koseki, Y., Toyoda, T., Okamura, K., Tajima, S., Mitsuya, K., Okano, M., Koseki, H., 2007. The SRA protein Np95 mediates epigenetic inheritance by recruiting Dnmt1 to methylated DNA. *Nature* 450, 908–912.
- Su, Y.-Q., Sugiura, K., Woo, Y., Wigglesworth, K., Kamdar, S., Affourtit, J., Eppig, J.J., 2007. Selective degradation of transcripts during meiotic maturation of mouse oocytes. *Dev. Biol.* 302, 104–117.
- Takeuchi, H., Yamamoto, M., Fukui, M., Inoue, A., Maezawa, T., Nishioka, M., Kondo, E., Ikeda, T., Matsumoto, K., Miyamoto, K., 2022. Single-cell profiling of transcriptomic changes during *in vitro* maturation of human oocytes. *Reprod. Med. Biol.* 21.
- Tang, F., Barbacioru, C., Nordman, E., Li, B., Xu, N., Bashkurov, V.I., Lao, K., Surani, M. A., 2010. RNA-Seq analysis to capture the transcriptome landscape of a single cell. *Nat. Protoc.* 5, 516–535.
- Wang, W., Qu, R., Dou, Q., Wu, F., Wang, W., Chen, B., Mu, J., Zhang, Z., Zhao, L., Zhou, Z., Dong, J., Zeng, Y., Liu, R., Du, J., Zhu, S., Li, Q., He, L., Jin, L., Wang, L., Sang, Q., 2021. Homozygous variants in PANX1 cause human oocyte death and female infertility. *Eur. J. Hum. Genet.* 29, 1396–1404.
- Wossidlo, M., Nakamura, T., Lepikhov, K., Marques, C.J., Zakhartchenko, V., Boiani, M., Arand, J., Nakano, T., Reik, W., Walter, J., 2011. 5-Hydroxymethylcytosine in the mammalian zygote is linked with epigenetic reprogramming. *Nat. Commun.* 2, 241.
- Wu, D., 2022. Mouse oocytes, A complex single cell transcriptome. *Front. Cell Dev. Biol.* 10, 827937.
- Wu, Q.-J., Zhang, T.N., Chen, H.H., Yu, X.F., Lv, J.L., Liu, Y.Y., Liu, Y.S., Zheng, G., Zhao, J.Q., Wei, Y.F., Guo, J.Y., Liu, F.H., Chang, Q., Zhang, Y.X., Liu, C.G., Zhao, Y. H., 2022. The sirtuin family in health and disease. *Signal Transduct. Targeted Ther.* 7, 402.
- Yan, R., Gu, C., You, D., Huang, Z., Qian, J., Yang, Q., Cheng, X., Zhang, L., Wang, H., Wang, P., Guo, F., 2021. Decoding dynamic epigenetic landscapes in human oocytes using single-cell multi-omics sequencing. *Cell Stem Cell* 28, 1641–1656.e1647.
- Yanez, L.Z., Han, J., Behr, B.B., Pera, R.A.R., Camarillo, D.B., 2016. Human oocyte developmental potential is predicted by mechanical properties within hours after fertilization. *Nat. Commun.* 7, 10809.
- Yang, F., Wang, W., Cetinbas, M., Sadreyev, R.I., Blower, M.D., 2020. Genome-wide analysis identifies cis-acting elements regulating mRNA polyadenylation and translation during vertebrate oocyte maturation. *RNA* 26, 324–344.
- Yoder, J.A., Soman, N.S., Verdine, G.L., Bestor, T.H., 1997. DNA (cytosine-5)-methyltransferases in mouse cells and tissues. Studies with a mechanism-based probe. *J. Mol. Biol.* 270, 385–395.
- Yu, B., Dong, X., Gravina, S., Kartal, O., Schimmel, T., Cohen, J., Tortoriello, D., Zody, R., Hawkins, R.D., Vijg, J., 2017. Genome-wide, single-cell DNA methylomics reveals increased non-CpG methylation during human oocyte maturation. *Stem Cell Rep.* 9, 397–407.
- Yu, B., Doni Jayavelu, N., Battle, S.L., Mar, J.C., Schimmel, T., Cohen, J., Hawkins, R.D., 2020. Single-cell analysis of transcriptome and DNA methylome in human oocyte maturation. *PLoS One* 15, e0241698.
- Zhao, H., Li, T., Zhao, Y., Tan, T., Liu, C., Liu, Y., Chang, L., Huang, N., Li, C., Fan, Y., Yu, Y., Li, R., Qiao, J., 2019. Single-cell transcriptomics of human oocytes: environment-driven metabolic competition and compensatory mechanisms during oocyte maturation. *Antioxidants Redox Signal.* 30, 542–559.